JOURNAL OF GEOPHYSICAL RESEARCH, VOL. 113, A10201, doi:10.1029/2008JA013157, 2008

Magnetospheric amplification and emission triggering by ELF/VLF waves injected by the 3.6 MW HAARP ionospheric heater

M. Gołkowski,[1] U. S. Inan,[1] A. R. Gibby,[1] and M. B. Cohen[1]

Received 10 March 2008; revised 2 June 2008; accepted 26 June 2008; published 1 October 2008.

[1] The HF dipole array of the High Frequency Active Auroral Research Program (HAARP) in Gakona, Alaska, was recently upgraded to 180 elements, facilitating operations at a total radiated power level of 3.6 MW and an effective radiated power of ~575 MW. In the first experiments at the new power level, the HAARP array is used for magnetospheric wave injection. Modulated heating of auroral electrojet currents in the ionosphere yields radiation in the ELF/VLF frequency range. The HAARP-generated signals are injected into the magnetosphere, where they propagate in the whistler mode in field-aligned "ducts," allowing them to be observed at the conjugate point on a ship-borne receiver and on autonomous buoy platforms. The observation of the 1-hop signals is accompanied by the observation of associated 2-hop components in the northern hemisphere, which have reflected from the ionospheric boundary in the southern hemisphere. The observed signals are accompanied by triggered emissions and exhibit temporal amplification of 15–25 dB/s and bandwidth broadening to ~50 Hz. Amplification occurs at injected signal frequencies selected in near real time on the basis of observations of natural emission activity, and only certain components of the frequency-time formats transmitted are amplified. Observations at multiple sites and dispersion analysis show that the signals are injected into the magnetosphere directly above the HF heater. The duration of echo observation and the prevalence of 1-hop observations are consistent with statistics from 1986 Siple Station experiments. The particle-trapping wave amplitude near the magnetic equator is estimated in the range 0.1–0.4 pT and gyroresonance with 10 keV–100 keV electrons.

Citation: Gołkowski, M., U. S. Inan, A. R. Gibby, and M. B. Cohen (2008), Magnetospheric amplification and emission triggering by ELF/VLF waves injected by the 3.6 MW HAARP ionospheric heater, *J. Geophys. Res.*, *113*, A10201, doi:10.1029/2008JA013157.

1. Introduction

[2] Controlled wave injection experiments allow quantitative investigation of magnetospheric whistler mode wave particle interactions. The dimensions and characteristic scales of the interactions dwarf any feasible laboratory setup while observations of naturally occurring emissions inherently lack repeatability. On the other hand, generation of ELF/VLF frequencies (500 Hz to 6 kHz) required for magnetospheric gyroresonance experiments poses a significant engineering problem owing to the multi-kilometer scale of the free-space wavelengths involved. The pioneering experiments conducted with the Siple Station, Antarctica transmitter during 1973–88 documented many characteristics of wave growth and triggering and continue to serve as a foundation for theoretical studies [*Helliwell*, 1988]. The Siple Station experiment in its final version consisted of a 150 kW transmitter driving 42 km crossed dipoles constructed on a ~2 km thick ice sheet. The operating frequency range of the Siple transmitter was ~1–8 kHz but transmissions required tuning of the antenna, which limited the operable bandwidth to ~500 Hz. Furthermore, few transmissions were conducted at frequencies below 2 kHz owing to the low antenna efficiency and operational power limitations at these frequencies. Even with its impressive physical dimensions and unique location, the ELF/VLF radiation efficiency of the Siple transmitter antenna was at most ~3% and even lower at low frequencies.

[3] The newly upgraded HAARP facility offers the potential to continue and expand magnetospheric wave injection research by generating ELF/VLF waves via modulated HF heating of ionospheric currents. Modification of the conductivity of the ionospheric plasma with HF waves and thus the use of natural overhead current systems as an ELF/VLF antenna in the sky was first reported by *Getmantsev et al.* [1974]. Extensive work was subsequently carried out by the European Incoherent Scatter (EISCAT) Scientific Association using the 1 MW heating facility in Tromsø, Norway [*Stubbe et al.*, 1982; *Barr and Stubbe*, 1984, 1991; *Rietveld et al.*, 1987, 1989]. The High Fre-

[1]STAR Laboratory, Department of Electrical Engineering, Stanford University, Stanford, California, USA.

0148-0227/08/2008JA013157$09.00

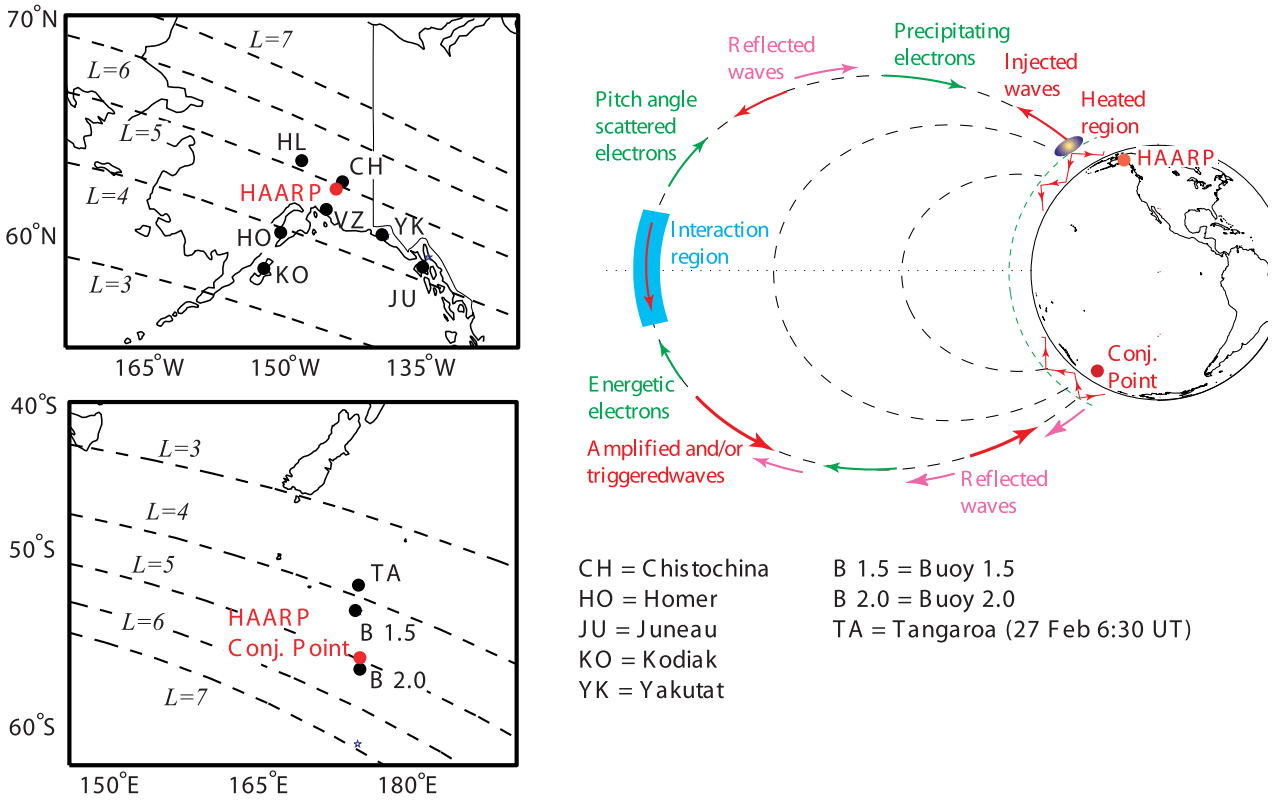

Figure 1. Maps showing the locations of ground-based receiver sites in the northern and southern hemispheres as well as a cartoon illustrating ducted whistler mode propagation excited by the HAARP HF heater.

quency Active Auroral Research Program (HAARP) heating facility in Gakona, Alaska was completed in 1996 with a 960 kW radiated power. Several characteristics of HAARP make it an ideal test bed for magnetospheric wave injection experiments. Unlike the Tromsø heater, HAARP is located at ($L \simeq 4.9$) on sub-auroral (closed) field lines allowing for hemisphere to hemisphere ducting [*Carpenter and Šulić*, 1988]. The location of HAARP is also particularly advantageous for the conduct of magnetospheric ELF/VLF wave-injection experiments. Previous experiments at Siple Station [*Helliwell and Katsufrakis*, 1974] mainly probed the regions of $L \simeq 4.2$ on field lines primarily inside the plasmasphere. HAARP, on the other hand, is located at a higher latitude, allowing for injections both inside and outside the plasmasphere and is thus well suited for probing of the irregularity-rich plasmapause region. Moreover, the effective frequency range of HAARP spans from a few Hz to 30 kHz and is not limited by antenna tuning, so that whistler mode wave-injection experiments can be conducted over a much wider frequency range.

[4] The first observations of HAARP induced magnetospherically amplified signals were reported by *Inan et al.* [2004] and included local and conjugate observations of signals in the 1–2 kHz range and associated triggered emissions. In February 2007 the radiated power of HAARP was upgraded to 3.6 MW, making it the most powerful HF heater in the world. We report here the results of the first set of magnetospheric wave injection experiments with the 3.6 MW HAARP facility.

2. Experimental Setup

2.1. Northern Hemisphere

[5] The HAARP facility is located at ~62.4°N and 145.2°W geographic (63.1°N and 92.4°W geomagnetic). The HF heater consists of 180 crossed dipoles arranged in a 12 by 15 rectangular array capable of a total radiated power of 3.6 MW and effective radiated power (ERP) of ~575 MW. HF carrier frequencies ranging from 3 to 9 MHz are available and ELF formats can be impressed upon the carrier using up to 100% sinusoidal amplitude modulation. The cartoon in Figure 1 illustrates the injection of HAARP ELF signals into the magnetosphere and the propagation of these signals to the conjugate southern hemisphere within field-aligned ducts. When observed in the southern hemisphere, the signals are known as "1-hop" echoes. If the signals experience a partial reflection from the lower ionospheric boundary in the southern hemisphere and are subsequently received in the north, they are referred to as "2-hop" echoes. Subsequent reflections and crossings of the magnetic equator are denoted with a correspondingly higher hop number. The local HAARP-generated ELF signals and also 2-hop echoes are measured with a constellation of 9 ELF/VLF receiver sites as shown in Figure 1. The receivers are Stanford AWESOME (Atmospheric Weather Educational System for Observation and Modeling

of Effects) receivers and utilize large square (4.8 m by 4.8 m) or triangular (4.2 m high with 8.4 m base) air core antennas, with terminal resistive and inductive impedances respectively of 1-Ω and 1-mH, matched to a low-noise (noise figure of ∼2–3 dB at a few kHz) preamplifier with a flat frequency response (∼300 Hz to ∼40 kHz). The receiver closest to HAARP is located at Chistochina at a distance of 37 km from the facility, while the more distant sites of Kodiak and Juneau are at distances of ∼700 km. The spatial spread of the receivers allows for detection and geo-location of echoes using the methods described by *Gołkowski and Inan* [2008]. Although magnetospheric injection is expected to be most favorable directly above the heater, HAARP ELF signals travel in the Earth-ionosphere wave-guide up to thousands of kilometers [*Moore et al.*, 2007] and can thus in principle be coupled upward into the magnetosphere at considerable distances from the heater.

[6] A wide range of ELF formats including pulses, frequency-time ramps and chirps are utilized to probe the magnetospheric plasma with HAARP transmissions. All of the receiver sites are equipped with Internet connectivity and send 1 min spectrograms in real time to a server at Stanford University. Monitoring of the HAARP ELF signals, natural conditions, and echo observations allow for real-time evaluation of the experimental conditions. Using an Internet chat room to communicate with the HAARP operator, transmissions can be modified to respond to changing conditions. Similar real-time adjustment of transmitter parameters based on observations of natural signals and echoes was also used with success during the Siple experiments [*Helliwell and Katsufrakis*, 1974].

2.2. Southern Hemisphere

[7] The magnetic conjugate point of HAARP is located 1000 km from the nearest landmass in the Southern Pacific Ocean. For ELF/VLF measurements at this remote location, we use two autonomous buoy-based receiving systems deployed by Stanford University, designated Buoy 1.5 (an upgrade of an earlier version) and Buoy 2.0. The map of the southern hemisphere in Figure 1 shows the locations of both buoys, which were chosen to provide a spread in latitude and longitude around the HAARP conjugate point. Buoy 1.5 and Buoy 2.0 each contain a 3 channel VLF receiver with air-core antennas with 5.8 m^2 and 3.3 m^2 areas, respectively. Both systems are remotely controlled and transmit data via IRIDIUM satellite modem. Power requirements are met with a large battery bank and photovoltaic solar panels. Owing to limitations of data storage and transmission bandwidth the buoys only take synoptic recordings of 1 min every 15 min. Since the HAARP campaign described herein coincided with the deployment of both buoys, additional VLF recordings were made on board the ship R/V Tangaroa, which was used for deployment of the buoys. The ship-borne receiver is of the same type used at the Alaska sites as mentioned above.

3. Observations

3.1. The 27 February 2007 Observations

[8] The HAARP array transmitted continuously for 7 hours a day (0000–0700 UT) from 26 February to 4 March 2007. The primary HF frequency utilized was 3.25 MHz with additional transmissions attempted at HF frequencies up to 9.0 MHz. During the 7 day campaign, whistler mode echoes were observed only on 27 February and 4 March. At the time of the 27 February observations, the HAARP transmission format contained sequences of single frequency pulses, frequency-time ramps and chirps, and a continually increasing frequency-time signature with sinusoidal segments called a "snake" ramp. The full frequency range of the format was 1 to 5 kHz and the repetition period of the format was 60 s. The modulation format was impressed upon a 3.25 MHz carrier frequency using 100% sinusoidal modulation. Figures 2a–2c show three spectrograms from the northern hemisphere. Figures 2d and 2e show the simultaneous and later minutes from the southern hemisphere observed on Tangaroa. The time of the observation is before the deployment of the two buoys so the receiver on Tangaroa was the only one available in the southern hemisphere. A portion of the "snake" ramp is the only part of the transmission format that exhibited clear repeatable magnetospheric amplification and inter-hemisphere propagation even though other signals in the same frequency range were transmitted. In Figure 2a, showing data from Chistochina (35 km from HAARP), the locally observed, HAARP-transmitted snake ramp is clearly visible between 50 and 60 s. Beginning at 58 s the 1-hop echo is observed on Tangaroa, seen in Figures 2d and 2e. While the Tangaroa spectrogram in Figure 2d shows the simultaneous minute of the northern hemisphere records, Figure 2e is from 7 min later and is evidence of the repeatability of the phenomenon. Although the snake ramp echo is accompanied by triggered emissions and appears much more diffuse than its locally observed, HAARP-generated parent, the frequency range and periodicity of the conjugate observations (i.e., occurrence in the same second of each minute), is clear evidence of their causative triggering by the HAARP transmissions of 1 min periodicity. The amplitudes of the locally observed HAARP signal at Chistochina is in the range 0.14 to 0.16 pT for elements below 2 kHz and 0.29 to 0.30 pT above 2 kHz. The enhancement in amplitude above 2 kHz is a product of the Earth-ionosphere waveguide resonance [*Stubbe et al.*, 1982]. However, only the elements below 2 kHz trigger 1-hop echoes, whose amplitude on Tangaroa is 0.19–0.27 pT. Careful examination of the records revealed that 1 s pulses at 1225 Hz and a 500 Hz/s frequency-time ramp also triggered faint 1-hop echoes, as shown in Figure 2. These are, however, weaker and less consistent than those triggered by the snake ramp.

[9] No 2-hop echoes are observed in the northern hemisphere at any sites. At the time of observation, Tangaroa was located at 52.4° S and 174.8° E geographic and 58.8° S and 265.37° E geomagnetic yielding an L shell of 3.8 using an IGRF model of the geomagnetic field. The Kodiak station is on the same magnetic longitude (265.17°) as Tangaroa although equatorward of its conjugate point at an L shell of 3.4. The remaining sites were at higher L shells, and at substantial distances away in longitude, being located >200 km from the Tangaroa conjugate point. Examination of the spectrograms from Kodiak and Juneau shows that in the frequency range below 2 kHz for which echoes are observed, the HAARP-generated signals did not subionospherically propagate to these sites, and therefore would not have been injected into the magnetosphere above

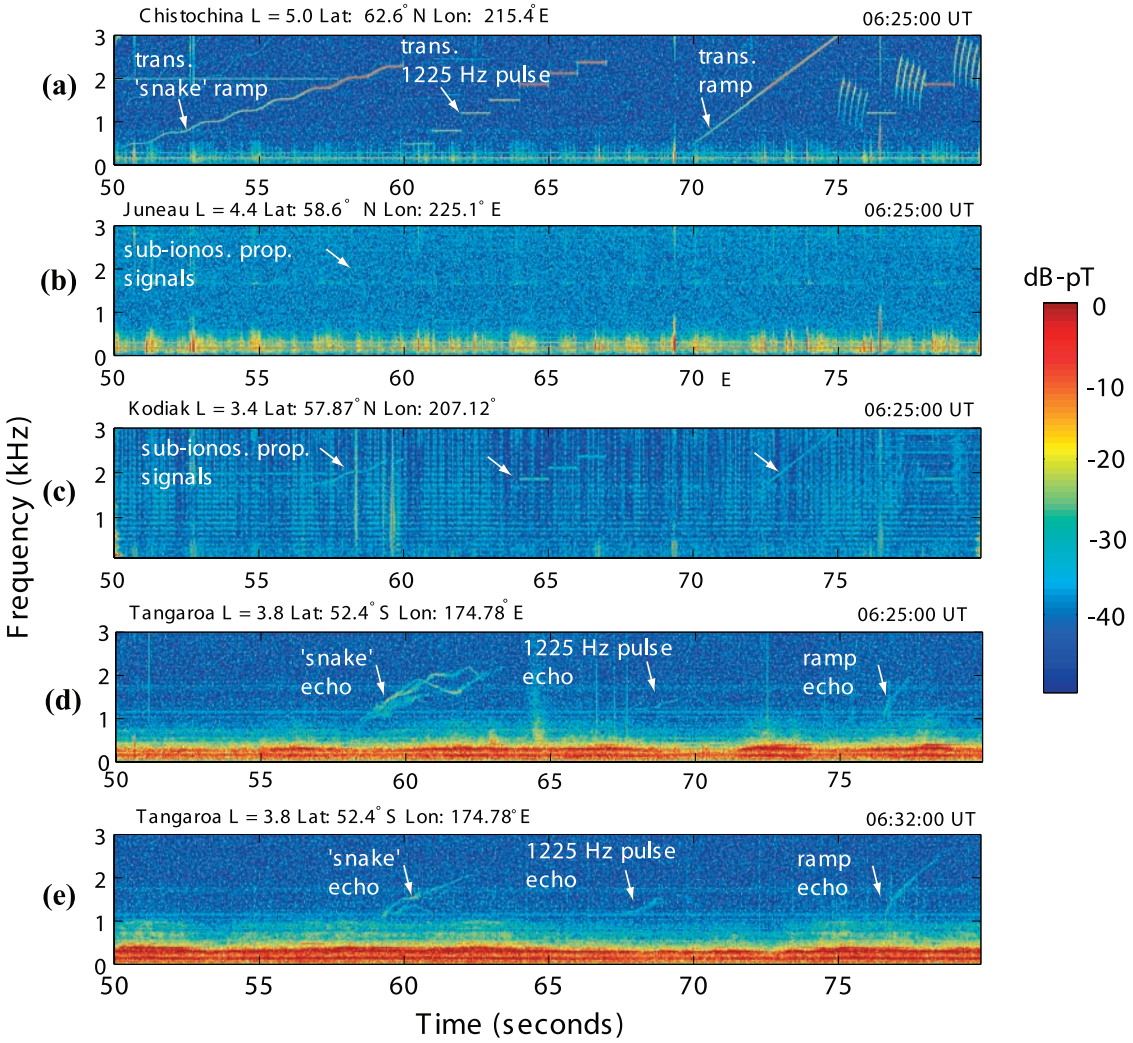

Figure 2. Spectrograms showing (a–c) HAARP-generated ELF signals at three sites in the northern hemisphere and (d and e) 1-hop echoes of 3 different HAARP signals observed in the southern hemisphere. Only signals above 2 kHz are observed to propagate to long distances (~700 km) from the HAARP facility in the Earth ionosphere waveguide.

these locations. The higher amplitudes of subionospherically propagating signals at Kodiak as compared to Juneau are addressed in a report by *Cohen et al.* [2008]. The hypothesis that the signal was injected into the magnetosphere in the vicinity of the HAARP heater is confirmed by dispersion analysis. Two of the echoes from the 500 Hz/s frequency-time ramp spanned a frequency range (0.7–2 kHz) broad enough to allow for determination of the L shell of propagation and the equatorial cold plasma density using whistler-dispersion techniques [*Sazhin et al.*, 1992, and references therein]. The results are summarized in Table 1, and were obtained using a two-parameter optimization algorithm for fitting a theoretical dispersion curve (including both ionospheric and magnetospheric dispersion) to the observation for four versions of the diffusive equilibrium model [*Angerami and Carpenter*, 1966]. Figure 3 shows an overlay of the dispersion curve corresponding to the DE-1 model thought to be the most reasonable estimate given the magnetospheric density profile derived from *Carpenter and Anderson* [1992] discussed in section 4.1.

[10] The HAARP facility is located at L = 4.95 (IGRF model) so the above dispersion results and their implication of injection directly above the heater, show agreement with recent satellite measurements of HAARP signal injection into the magnetosphere showing a high-amplitude upward column of radiation concentrated in a region of ~30 km diameter directly above the heater [*Piddyachiy et al.*, 2008], and also a recent theoretical model of ELF/VLF radiation from modulated ionospheric currents, which shows a similar overhead columnar excitation [*Lehtinen and Inan*, 2008]. We thus conclude that the echoes observed on Tangaroa traveled in a duct at around L ~ 4.95–5.0 similar to the echoes observed by *Inan et al.* [2004]. The lack of echo observations in the northern hemisphere agrees with statistical results from Siple Station that are discussed in section 4.1 and show much higher likelihood for 1-hop observations over 2-hop observations.

[11] The observation of the echoes on 27 February persisted for 20 min from 0620–0640 UT, with varying intensity of the echoes exhibiting two maxima at 0626 and 0635 UT. Figure 4 shows the amplitude of the HAARP

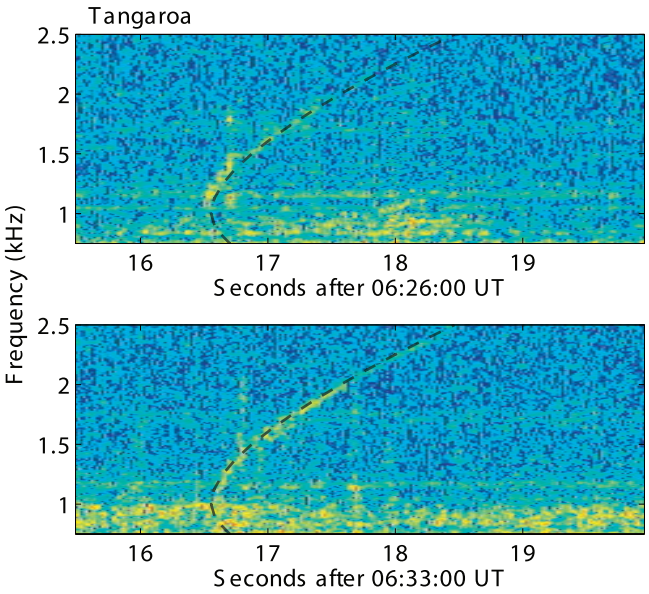

Figure 3. One-hop echoes of 500 Hz/s frequency-time ramp with overlay of theoretical dispersion (dotted black line) corresponding to the DE-1 model presented in Table 1.

signals observed at Chistochina, the amplitude of the echoes on Tangaroa and the deviations from an hourly average of three components of the Earth's magnetic field from a magnetometer at the HAARP site, which gives a measure of the electrojet strength and direction. These maxima of echo intensity show good correlation with the amplitudes of HAARP signals at 1875 Hz observed locally at Chistochina which themselves exhibit strong correlation with the north–south horizontal (H) component of the geomagnetic field. It is worth noting that in general the relationship between magnetometer readings and HAARP ELF radiation is not straightforward and the close correlation seen here is not always observed [*Cohen et al.*, 2008]. The magnetometer readings suggest that the increased HAARP signal strength is due to an increase in electrojet intensity and not a change in direction. However, at 0645 UT the local HAARP ELF intensity and the electrojet intensity (north–south horizontal component) exhibit a third maximum of equal amplitude during which no further echoes were observed on the ship. Thus although the strength of HAARP ELF radiation clearly plays a role in echo observations, other processes are at work and are discussed in section 4.1.

3.2. The 4 March 2007 Observations

[12] On 4 March 2007, echoes of 3 s pulses at 1100 Hz were observed in both hemispheres on Buoy 1.5 and 2.0 and at Chistochina. Observation of the 2-hop echoes abruptly commenced when the transmission format was changed at 0617 UT from one with parabolic chirps and 1 s duration 1225 Hz pulses, to a format with 3 s 1100 Hz pulses, 1 s 900 Hz and 1600 Hz pulses, and a frequency-time ramp from 500 Hz to 3 kHz, as shown in Figure 5. Figure 5 (left) shows that no echoes are observed from the first format, while Figure 5 (right) shows a clear echo with triggered emissions from the 3 s long pulse at 1100 Hz in the second format. Figure 6 shows spectra from the 0625 minute observed at Chistochina (Figure 6, top), on Buoy 1.5 (Figure 6, middle), and from the 0620 minute on Buoy 2.0 (Figure 6, bottom). The data from Buoy 2.0 are compromised by impulsive interference radiated from the system electronics and manifested as vertical lines in the spectrum. The source of the interference is believed to be sparking in a faulty battery terminal. The data in Figure 6 (bottom) has been processed using noise subtraction and echoes and triggered emissions are visible in between the remaining impulsive interference. All three panels in Figure 5 show that the magnetospheric echoes are triggered primarily by the 3 s long pulses even though shorter pulses at 900 Hz and 1600 Hz as well as a 500 Hz/s frequency-time ramp are also transmitted at this time. A detailed examination of the records, reveals that a few of the 900 Hz pulses also yield faint echoes and triggered emissions, marked by arrows at 29 and 49 s in Figure 5 (middle), though no evidence of echoes was found for the 1600 Hz pulses or the frequency-time ramp. While the 1-hop echoes at 1100 Hz are primarily 3 s long pulse-like signals with additional off frequency triggered emissions, the 2-hop echoes consist of only the initial portion of the original 3 s long HAARP-transmitted pulses. The duration of observation of the echoes on this day was 0617 to 0630 UT for 2-hop echoes at Chistochina and the 0620 and 0625 synoptic minutes for 1-hop echoes on Buoy 2.0 and Buoy 1.5, respectively (not observed at 0610, 0615, 0635, or 0640). Unlike the 27 February observations, on 4 March the HAARP signal amplitudes showed very little variation during the echo observation time. The 1-hop echoes exhibit growth and amplitude variation but can be characterized with typical amplitude values of 0.04–0.06 pT on Buoy 1.5 and 0.03–0.05 pT on Buoy 2.0. The two buoys did not record simultaneously, and were separated ~280 km in distance. The 2-hop echoes at Chistochina showed much more variation than the 1 hop echoes even over 10 s (period of consecutive transmissions at 1100 Hz) with maximum amplitudes of ~0.15 pT and minimum amplitudes falling into the noise floor of ~0.01 pT. The 1-hop echoes were not observed on Tangaroa, 60 km away northwest of Buoy 1.5. However, we note that the noise floor on Tangaroa was variable and at the time of the 4 March observations was ~0.1 pT. Superposed epoch analysis to extract signals from the noise did not yield any evidence of HAARP signals in Tangaroa data. In the northern hemisphere, the echoes were primarily observed at Chistochina although some of the higher-amplitude triggered emissions were also observed at Valdez and Healy at distances of 135 and 234 km from HAARP, respectively.

[13] The observation of single frequency echoes on 4 March allows for quantification of temporal amplification resulting from the magnetospheric wave-particle interaction. Such a calculation is less useful for more complicated frequency-time formats such as the "snake" ramp since

Table 1. Dispersion Analysis Results

Model	Electron Temp. (K)	Composition at 1000 km			*L* Shell	N_{eq} (cm^{-3})
		O^+	H^+	He^+		
DE-1	1600	90%	8%	2%	4.99	396
DE-2	3200	90%	8%	2%	4.97	430
DE-3	1600	50%	40%	10%	4.99	397
DE-4	800	50%	40%	10%	5.05	325

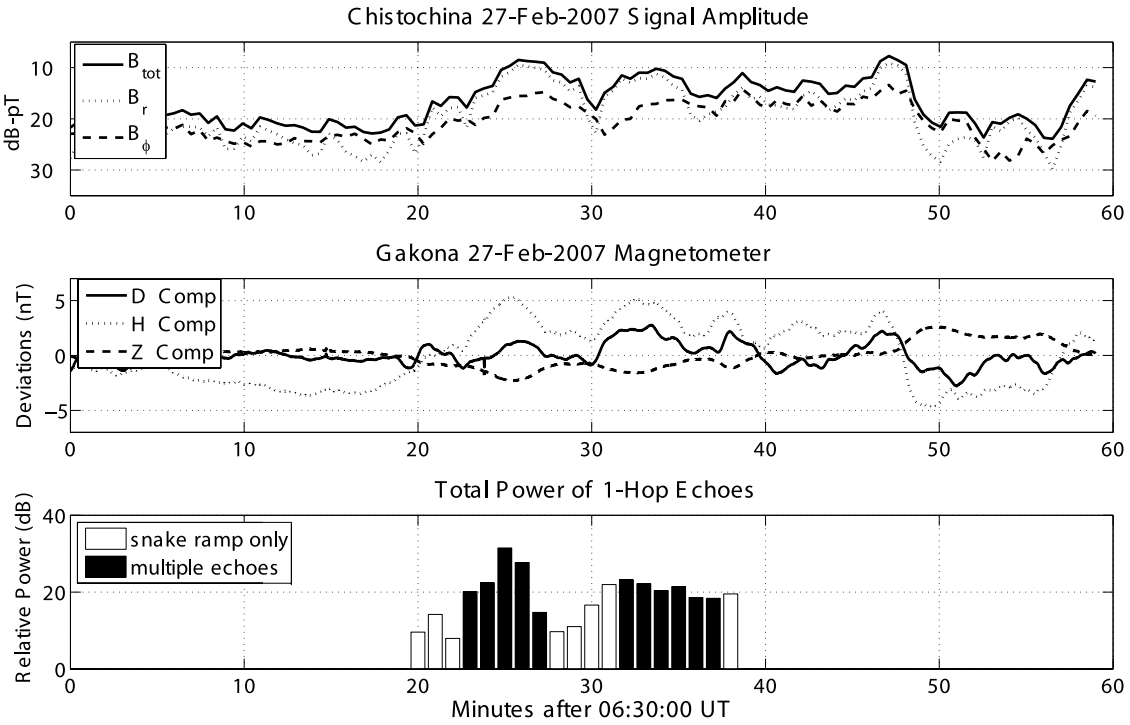

Figure 4. (top) Local HAARP ELF signal strength at Chistochina as observed in the amplitude of the radial magnetic field (B_r), the azimuthal magnetic field (B_ϕ), and the total magnetic field (B_{tot}). (middle) Variations of the geomagnetic field from a magnetometer at the HAARP site with positive northward component (H), positive eastward component (D), and positive downward component (Z). (bottom) Relative integrated power of echoes observed on Tangaroa. All three panels show maxima at 0626 and 0635, although no echoes are observed during the third maximum in signal power and electrojet strength at 0646.

the frequency response of the HAARP ELF generation process in the context of magnetospheric injection is not known. Figures 7a and 7b show the amplitudes of the 3 s pulse 1-hop and 2-hop echoes, respectively, using a 100 Hz band-pass digital filter. Several 1-hop echoes experienced ~15 dB/s temporal amplification for 2 s before reaching saturation and triggering emissions. The amplitudes of the 2-hop echoes show ~25 dB/s growth for a second, with subsequent triggering of emissions. Additional aspects of the wave-particle interaction are manifested in the bandwidth broadening of the pulses to ~50 Hz and of the shift of the central frequency by 10 Hz to 1110 Hz (Figures 7c and 7d) similar to that reported by *Stiles and Helliwell* [1975] in their spectral analysis of whistler mode echoes excited by VLF transmitters.

[14] Examination of the individual echoes observed on Buoy 1.5 shows that while most of the echoes exhibited temporal growth followed by saturation and triggering of emissions as mentioned above, at least one of the echoes was composed primarily of emissions initially triggered by

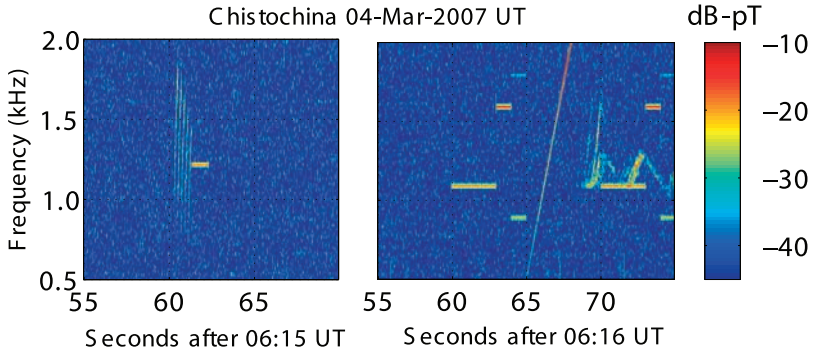

Figure 5. Change of HAARP transmission format seen in data from Chistochina. Format with parabolic chirps and 1 s pulses at 1225 Hz was terminated at 0616. Format with 3 s pulse at 1100 Hz, 1 s pulses at 1600 Hz and 900 Hz and 500 Hz to 3.0 kHz frequency-time ramp commenced at 0617. The first 3 s pulse at 1100 Hz triggered a 2-hop echo starting at 0617:08.

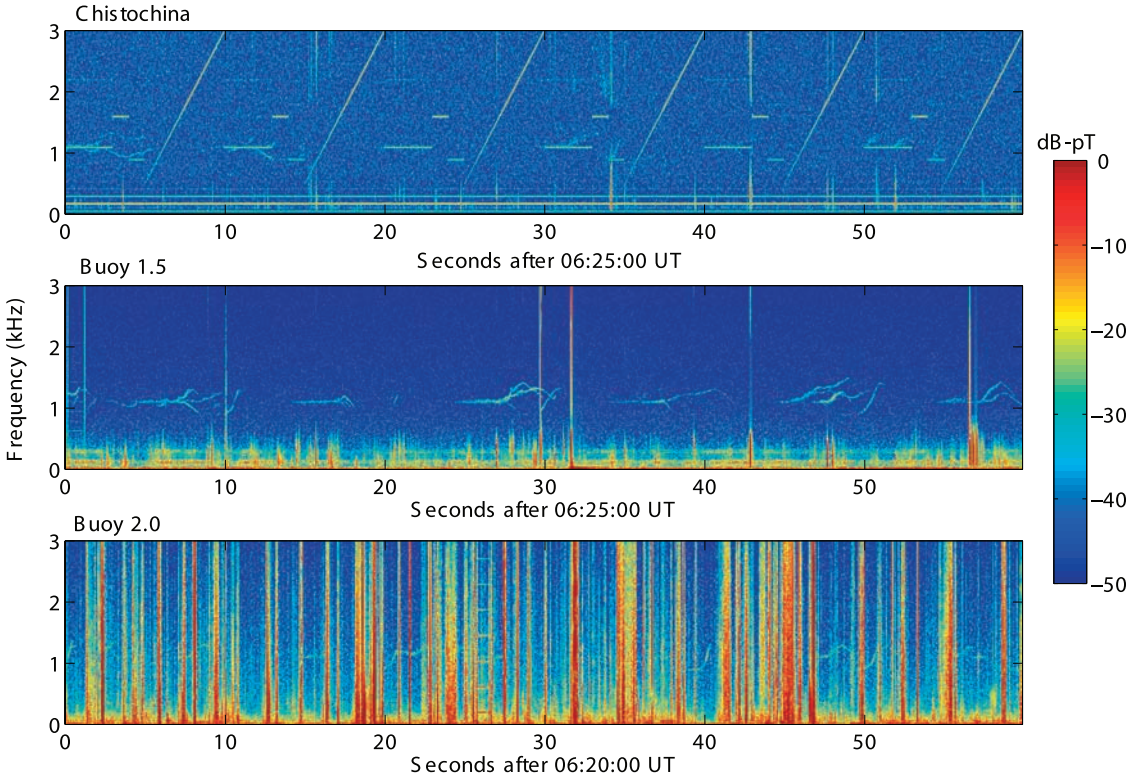

Figure 6. (top) HAARP transmission and faint 2-hop echoes at Chistochina and (middle) clear 1-hop echoes observed simultaneously on Buoy 1.5. (bottom) Echoes observed on Buoy 2.0 five min earlier. The 2-hop echoes at Chistochina (top panel) appear superimposed on consecutive HAARP transmissions of the same frequency since the 2-hop propagation time and format repetition period are comparable, being 8.4 and 10 s, respectively.

the previous echo entrained by the transmitted pulse. Entrainment is a non-linear phenomena of magnetospheric wave-particle interactions in which a triggered emission interacts with a coherent wave causing the normally free-running frequency-time behavior of the emission to follow that of the coherent wave [*Helliwell*, 1988]. Figure 8 shows a side-by-side comparison of two echoes observed on Buoy 1.5. While the echo in Figure 8b, whose amplitude is shown in Figure 8d, shows steady temporal amplification from a level below the noise floor, the echo in Figure 8a (amplitude

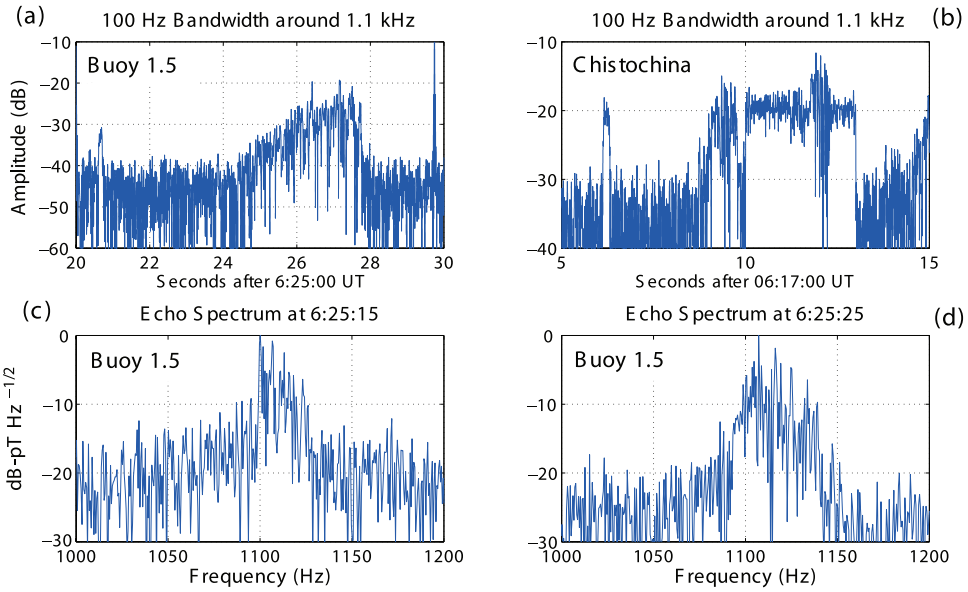

Figure 7. Temporal amplification and frequency spreading of 1100 Hz pulses observed on Buoy 1.5.

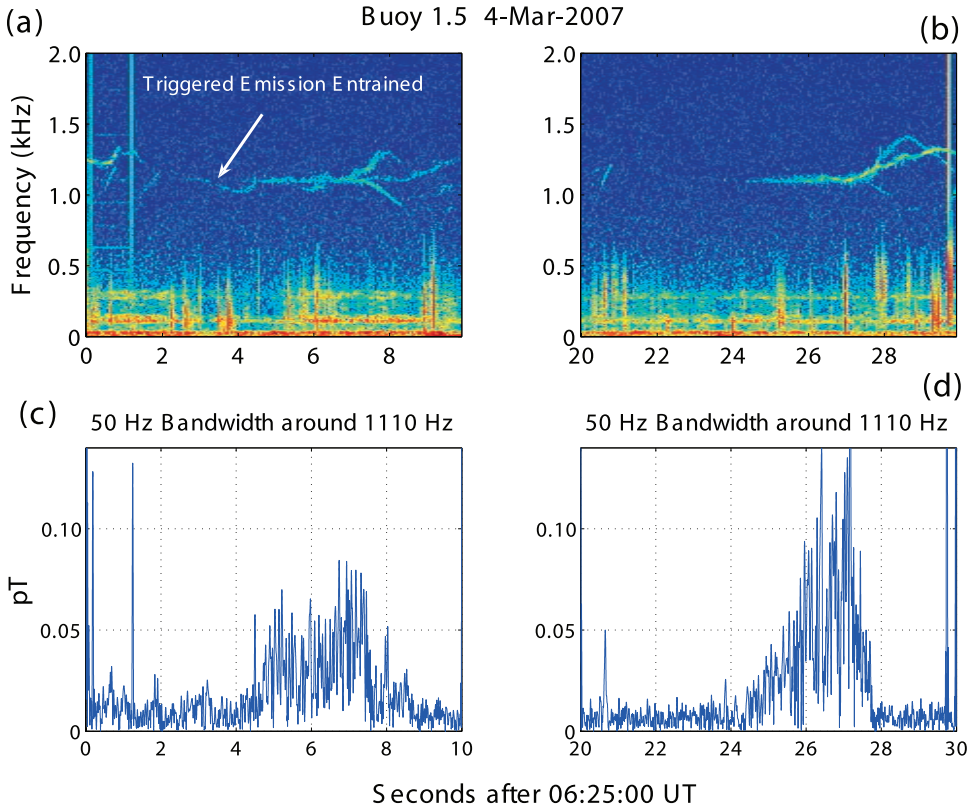

Figure 8. (a) One-hop echo on Buoy 1.5 exhibiting entrainment of emission triggered by previous echo, contrasted with (b) a 1-hop echo on Buoy 1.5 exhibiting temporal amplification and triggering of emissions without entrainment. (c and d) The amplitude within a 50 Hz bandwidth of the central frequency of the echoes in Figures 8a and 8b, respectively.

in Figure 8c) shows a substantial initial amplitude and is connected to the triggered emission from the previous echo.

4. Interpretation

4.1. Conditions and Time Scales for Observations of HAARP-Induced Whistler Mode Echoes

[15] In most cases when echoes are observed, two parameters that can readily be determined are the magnetospheric propagation path and the associated equatorial cold plasma density. The 1-hop propagation time for the 4 March pulse echoes was ~4.2 s, very similar to the ~4 s propagation time from previous observations of HAARP echoes made by *Inan et al.* [2004], in which dispersion analysis allowed for the direct determination of the L shell of propagation ($L \simeq 4.9$) and equatorial electron density ($N_{eq} \simeq 280$ cm^{-3}). The *Inan et al.* [2004] observations inferred magnetospheric injection of the HAARP signals directly above the HAARP heater and magnetospheric propagation just inside the plasmapause boundary. For the 4 March case, accurate dispersion analysis is not possible owing to the single frequency of the pulse echoes. However, taking advantage of multiple receiver locations in the northern hemisphere it is still possible to draw conclusions about the magnetospheric path. *Tsuruda et al.* [1982] showed that whistler mode signals coupled from the magnetosphere into the Earth-ionosphere waveguide exhibit high spatial attenuation of ~7 dB/100km. In this context, the lack of observations of the 4 March 2-hop echoes at sites other than Chistochina, suggests that the magnetospheric exit point is in the close vicinity of Chistochina and hence also the HAARP facility located 37 km southwest. In the southern hemisphere, the 1-hop echoes observed on Buoy 1.5 have higher average amplitudes than those observed on Buoy 2.0 five minutes earlier. The higher amplitudes on Buoy 1.5 would be consistent with an ionospheric exit point ~100 km equatorward of the HAARP conjugate point using the ~7 dB/100 km attenuation of *Tsuruda et al.* [1982], although we need to note that the two buoy recordings are not simultaneous. Likewise, multiple exit points in the southern hemisphere resulting from "unducting" at altitudes of ~1000 km are also possible as investigated by *Strangeways et al.* [1982] for whistlers. Suffice to say, on the basis of the above mentioned propagation time and multiple site results we conclude that the 4 March echoes propagated along $L \sim 4.9$ and through a similar cold plasma density as reported in *Inan et al.* [2004]. The 27 February "snake" ramp is also believed to have been injected into the magnetosphere in the close vicinity of the HAARP heater and propagated along $L \simeq 4.95$, $N_{eq} \simeq 400$ cm^{-3} as discussed in section 2 and shown in Table 1. It appears that all of the observed echoes have propagated through the

high-density region inside of the plasma pause boundary at an L shell of $\sim$4.9 with an equatorial electron density of $\sim$200–400 cm^{-3}. The above hypothesis and calculations are in agreement with the electron density profiles based simply on geomagnetic conditions using the formulations of *Carpenter and Anderson* [1992]. The Kp indices for 4 March show very quiet conditions with max Kp of 1 for the 36 hours preceding the observation. The observations of 27 February occurred in a deep lull between two periods of moderate activity. The Kp indices are 0 and 0+ for the 12 hours before the observation but as high as 3+ immediately before and after. On the basis of these values the plasmapause inner boundaries for 27 February and 4 March are derived to be at $L = 4.9$ and $L = 5.3$, respectively, although the former could easily be an underestimate of the local conditions since the *Carpenter and Anderson* [1992] formulations represent a coarse global average. These results are consistent with past studies which show magnetospheric amplification and triggering being observed predominantly within the plasmasphere [*Carpenter and Miller*, 1983; *Omura et al.*, 1991]. At this point, it is difficult to say whether propagation just inside the plasmapause is favorable for magnetospheric amplification because of the higher cold plasma densities or the presence of guiding structures.

[16] The amplitudes of the HAARP signals measured at Chistochina at the times of the echo observations were 0.03–0.2 pT, making them less than the typical values observed with the original HAARP array and much less than the maximum values of $\sim$3–5 pT observed with the upgraded array on other days of the campaign [*Cohen et al.*, 2008]. Thus, local HAARP signal strength does not seem to be the sole determining factor in exciting magnetospheric amplification. The relationship between HAARP ELF radiation as observed above (e.g., on satellites) and below (i.e., on the ground) the lower ionosphere is not well understood and could well exhibit an inverse relationship under certain conditions. In both of the cases presented here and those analyzed by *Inan et al.* [2004], observations of HAARP induced whistler mode echoes persist for only 20–30 min. The 27 February ''snake'' ramp observations illustrate that echo power is correlated to HAARP signal strength only within this short time window while the 4-March echo observations show no correlation to HAARP signal strength at all.

[17] To shed light on the conditions that are conducive to HAARP induced whistler mode echo observation, we rely on a statistical analysis of 1-hop and 2-hop echo receptions from the 1986 Siple Station experiments. In 1986, the Siple transmitter was operated 139 days of the year, spaced between March 1986 and January 1987, with the largest gaps in the data being May and September due to equipment issues. The ELF/VLF data in this period were recorded on analog magnetic tape at Siple Station and the conjugate point at Lake Mistissini in Québec, Canada. Recordings at Siple Station were made in a synoptic manner throughout the entire day. In contrast, recordings at Lake Mistissini were made in a continuous manner during periods in which the Siple facility was transmitting. All of the data from this period at both stations were digitized and 20 s spectrograms spanning 2–6 kHz were made and visually inspected for evidence of 1-hop and 2-hop echoes. A 1-hop reception was determined to have occurred if the Siple transmission was visibly detectable on the continuous spectrograms within a 2 min period. A 2-hop reception was determined to have occurred if the echo was visible during the :05,:20,:35, and :50 synoptic minutes which were common to all synoptic schemes used at Siple Station in 1986. The tabulated statistics were used to investigate the occurrence of 1-hop and 2-hop echo observations. Out of 7860 min of recordings at Siple Station during transmitter operations, 582 min contained 2-hop echoes yielding an observation percentage of $\sim$7%. At Lake Mistissini, on the other hand, 1-hop echoes were observed 10472 out of 27408 min yielding an observation percentage of $\sim$38%. These numbers imply that 1-hop observations are about 5 times more likely than 2-hop observations.

[18] The above direct comparison of the continuous and synoptic observation percentages needs to be understood in the context of the assumption that, statistically speaking, the synoptic recordings at Siple Station yield the same measurement of the 2-hop distribution as the continuous recordings at Lake Mistissini do of the 1-hop distribution. Since both sample sizes are sufficiently large, the only circumstance under which the assumption would not hold would be if the observations exhibited a preference for specific minutes of the hour, which is indefensible for a natural phenomenon. It is perhaps not surprising that 2-hop observations are more rare since they necessitate an appreciable reflection at the conjugate ionospheric boundary, coupling back into the guiding duct, and reamplification during a second equatorial crossing. The HAARP observations are consistent with the Siple results in that on 27 February only 1-hop echoes were observed and on 4 March the 2-hop echoes were more variable in amplitude and temporal length than the 1-hop echoes.

[19] The Siple statistics also quantify the expected duration of 1-hop and 2-hop echo observation. Figure 9 (left) shows a histogram of length of contiguous reception of 1-hop echoes in minutes, where contiguous is defined as not exhibiting gaps in echo reception longer than 4 min. Figure 9 (right) shows the same histogram for 2-hop observations with the exception that contiguous is defined as being observed in synoptic minutes spaced 15 min apart. Both histograms suggest that the 20-30 min durations of echo observation from HAARP are in agreement with the Siple experiment in that the latter shows that the majority of contiguous observations last less than 20 min. These times scales on the order of tens of minutes could be a result of changing duct geometry, which up to this point we have assumed to be fixed. Using phase and group delay measurements of whistlers, *Andrews et al.* [1978] showed that ducts can have observed cross L drifts of tens of meters per second at the equator, while more recently *Gołkowski and Inan* [2008] inferred more rapid drifts of duct exit points from chorus measurements. In this context, an investigation of the role of duct drift on echo observations is planned for a future experiment described in section 5.

[20] Even though the statistics from the Siple experiment are useful in providing a context for analysis of the new HAARP results, it is important to be aware of the differences between the two experiments. In addition to different magnetic latitudes ($L = 4.3$ for Siple, $L = 4.9$ for HAARP), the two facilities differ greatly in radiation power and pattern. For the original 960 kW HF HAARP array, radiated

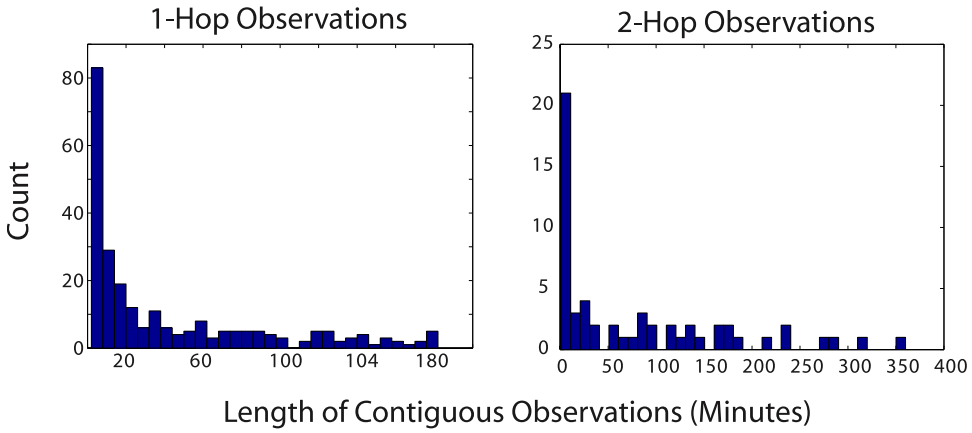

Figure 9. Histograms of contiguous observations of 1-hop and 2-hop signals of Siple signals from 1986. One-hop results are from continuous recordings at the Siple conjugate point; 2-hop results are from synoptic recordings at Siple Station taken 1 min out of every 15 min.

ELF power was estimated to range between 2 W and 30 W [*Moore et al.*, 2007; *Platino et al.*, 2006]. Assuming a best case linear scaling, the 3.6 MW HAARP array has a maximum ELF radiation power on the order of 100 W, compared to over 1 kW for the Siple transmitter [*Helliwell*, 1988]. Therefore, HAARP ELF waves injected into the magnetosphere are likely often close to the minimum threshold necessary for magnetospheric amplification on highly active paths[*Helliwell et al.*, 1980]. Furthermore, the Siple antenna radiated power directly into the Earth-ionosphere waveguide, where it would spread and leak into the magnetosphere at distances up to 200 km away from the transmitter [*Carpenter and Miller*, 1976; *Helliwell et al.*, 1980]. Since the altitude of the HAARP modulated electrojet dipole spans the lower ionospheric reflection height ($\sim$75–85 km), the coupling into the Earth-ionosphere waveguide and the radiation pattern injected into the magnetosphere is much more complicated. As previously mentioned, the HAARP radiation pattern into the magnetosphere is believed to be characterized by a narrow ($\sim$30 km) "column" geometry [*Lehtinen and Inan*, 2008; *Piddyachiy et al.*, 2008] which may reduce the chances of coupling energy (at levels that exceed the threshold of amplification) into ducts that are not directly overhead.

4.2. Frequency-Time Characteristics

[21] The two cases of observations illustrate that the dynamics of the wave-particle interaction are sensitive to both a finite frequency range and the specific frequency-time format of the injected signals. In the 4 March case, the fact that echoes were observed only after the change of pulse frequency from 1225 Hz to 1100 Hz implies that 1225 Hz lies above the "active" frequency range. Similarly, the very faint echoes of the 900 Hz pulses suggest that 900 Hz is close to the lower edge of the active range, which apparently spans no more than $\sim$300 Hz on this day. At the same time, lack of echoes from the frequency-time ramp which extended from 500 Hz to 3 kHz implies that the magnetospheric response is different for ramps and pulses. The importance of unique frequency-time formats is also exhibited in the 27 February echoes where many other signals transmitted in the frequency range that yielded favorable amplification for the "snake" ramp signal were not amplified. The specific frequency-time function of the "snake" ramp is

$$f(t) = 200t + 40\sin(5t) + 400 \qquad [\mathrm{Hz}] \tag{1}$$

[22] In their analysis of Siple data, *Carlson et al.* [1985] showed that magnetospheric amplification and triggering of emissions can be highly dependent on the slope of frequency-time ramps. The conventional understanding of the magnetospheric wave-particle interaction in the context of variable frequency waves is that spatial variations of the electron gyrofrequency match the Doppler-shifted wave frequency to first order [*Helliwell*, 1967]. More specifically, non-linear growth requires trapping of particles in the potential well of the input wave. *Nunn* [1974] derived the following expression for the collective inhomogeneity factor S for parallel propagating whistler mode waves interacting with energetic electrons. For simplicity we present a version developed by *Omura et al.* [1991].

$$S \equiv \frac{1}{\omega_t^2}\left[\left(3V_R - \frac{kv_\perp}{\Omega_e}\right)\frac{\partial\Omega_e}{\partial z} - \frac{2\omega + \Omega_e}{\omega}\frac{d\omega}{dt}\right] \tag{2}$$

where ω is the wave frequency, Ω_e is the electron gyroresonance frequency, k is the wave number, $v_\perp$ is the electron velocity perpendicular to the geomagnetic field, z is distance along a geomagnetic field line, and $V_R = (\omega - \Omega_e)/k$ is the electron resonance velocity. If $|S| < 1$ the electrons can be phase trapped in the wave potential well and oscillate with frequency approaching ω_t, also known as the trapping bandwidth, as S approaches 0. The trapping bandwidth is related to the wave amplitude B_w by

$$\omega_t \equiv \left(kv_\perp \frac{e}{m} B_w\right)^{1/2} \tag{3}$$

where e/m is the electron charge to mass ratio. Hence larger wave amplitudes, due to greater injection power or initial linear growth, relax the rigid gyroresonance condition put forth by *Helliwell* [1967]. The sensitive dependence of amplification on frequency-time format in the HAARP experiments is thus most likely related to the relatively low

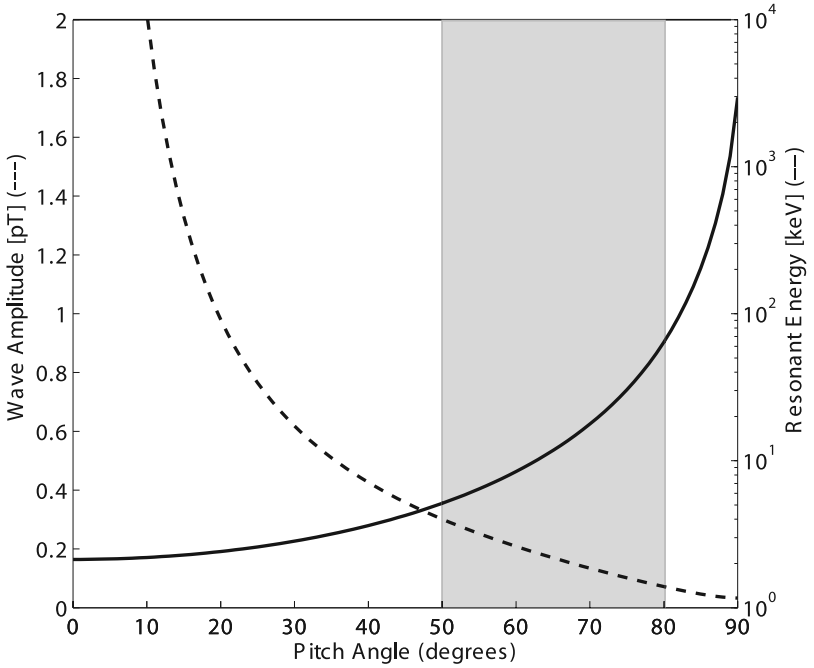

Figure 10. Resonant electron energies (solid line) and trapping wave amplitude (dashed line) versus equatorial pitch angle values. The input wave is a 1100 Hz parallel propagating wave traveling along L = 4.9 through a diffusive equilibrium cold plasma density model with equatorial electron density of 250 cm^{-3}. The shaded region corresponds to pitch angles between 50 and 80 degrees believed to be the main driver of the instability.

radiated ELF power of HAARP. Unfortunately, analytical analysis of the problem is limited in its usefulness owing to the dynamic nature of the system and fundamental unknowns such as the hot-plasma distribution. Since a comprehensive simulation is far beyond the scope of this work, we limit our analysis to estimating the trapping wave amplitude of the 1110 Hz pulse echoes observed on 4 March. Using the observed bandwidth broadening to 50 Hz, as illustrated in Figure 7, as a measure of the trapping bandwidth (ω_t), the calculation of trapping wave amplitude (B_w) proceeds from (4) with the necessity to assume a pitch angle and cold plasma density. On the basis of the propagation time, an equatorial electron density of 250 cm^{-3} at L = 4.9 is reasonable. We assume ducted propagation yielding wave normal angles parallel to the geomagnetic field. Figure 10 shows the resulting wave amplitudes and resonant electron energies versus pitch angle calculated at the geomagnetic equator. The shaded region in Figure 10 corresponds to high pitch angle $\alpha > 60^\circ$ electrons that likely drive the gyroresonance instability [*Bell et al.*, 2000]. The electrons involved in the amplification of the injected waves must have had energies ranging from a few tens to 100 keV with trapping wave amplitudes in the range 0.1–0.4 pT.

5. Summary

[23] Controlled wave-injection experiments with the upgraded HAARP facility have yielded new results of magnetospherically amplified signals. HAARP induced whistler mode echoes are observed during quiet magnetic conditions and propagate inside the plasmasphere. Propagation time and data from multiple sites point to magnetospheric injection in the close vicinity of the HAARP heater and propagation along a field-aligned path near L = 4.9. The 20–30 min duration of HAARP induced echo observations is found to be consistent with statistics from the 1986 Siple Station Experiment. The observations underline the significance of frequency-time signatures and "active" frequency ranges in the wave-particle interaction. Bandwidth broadening of the echoes allows for an estimate of the trapping wave amplitude at the magnetic equator of 0.1–0.4 pT and gyroresonance with 10–100 keV electrons. Further experiments that take full advantage of the dynamic capabilities of the HAARP facility are planned. In particular, probing the limits of coherence of the input wave on the instability is possible by transmitting signals with varying bandwidth or with frequency-time signatures that will arrive as wide band impulses at the equator. The role of duct drift in the observations will be investigated by observing the effects of aiming the HAARP HF beam at different positions in the ionosphere.

[24] **Acknowledgments.** This work was supported by the High Frequency Active Auroral Research Program (HAARP), by the Defense Advanced Research Programs Agency (DARPA), and by the Office of Naval Research (ONR) via ONR grant N0001405C0308 to Stanford University. Special thanks are due to the National Institute for Water and Atmospheric Research (NIWA) of New Zealand and the crew of R/V Tangaroa for their outstanding support during ship operations, to our hosts in Alaska, and to members of the Stanford VLF group for their help during the campaign.

[25] Amitava Bhattacharjee thanks Michael Starks and another reviewer for their assistance in evaluating this paper.

References

Andrews, M. K., F. B. Knox, and N. R. Thomson (1978), Magnetospheric electric fields and protonospheric coupling fluxes inferred from simulta-

neous phase and group path measurements on whistler mode signals, *Planet. Space Sci.*, *26*, 171–183.

Angerami, J. J., and D. L. Carpenter (1966), Whistler studies of the plasmapause in the magnetosphere: 2. Equatorial density and total tube electron content near the knee in magnetospheric ionization, *J. Geophys. Res.*, *71*(3), 711–725.

Barr, R., and P. Stubbe (1984), ELF and VLF radiation from the "polar electrojet antenna," *Radio Sci.*, *19*, 1111–1122.

Barr, R., and P. Stubbe (1991), ELF radiation from the Tromsø "super heater" facility, *Geophys. Res. Lett.*, *18*(6), 1035–1038.

Bell, T. F., U. S. Inan, R. A. Helliwell, and J. D. Scudder (2000), Simultaneous triggered VLF emissions and energetic electron distributions observed on POLAR with PWI and HYDRA, *Geophys. Res. Lett.*, *27*, 165–168.

Carlson, C. R., R. A. Helliwell, and D. L. Carpenter (1985), Variable frequency VLF signals in the magnetosphere: Associated phenomena and plasma diagnostics, *J. Geophys. Res.*, *90*(A2), 1507–1521.

Carpenter, D. L., and R. R. Anderson (1992), An ISEE/whistler model of equatorial electron density in the magnetosphere, *J. Geophys. Res.*, *97*, 1097–1108.

Carpenter, D. L., and T. R. Miller (1976), Ducted magnetospheric propagation of signals from the Siple, Antarctica, VLF transmitter, *J. Geophys. Res.*, *81*(16), 2692–2700.

Carpenter, D. L., and T. R. Miller (1983), Rare ground-based observations of Siple VLF transmitter signals outside the plasmapause, *J. Geophys. Res.*, *88*(A12), 10,227–10,232.

Carpenter, D. L., and D. M. Šulić (1988), Ducted whistler propagation outside the plasmapause, *J. Geophys. Res.*, *93*(A9), 9731–9742.

Cohen, M. B., M. Gołkowski, and U. S. Inan (2008), Orientation of the HAARP ELF ionospheric dipole and the auroral electrojet, *Geophys. Res. Lett.*, *35*, L02806, doi:10.1029/2007GL032424.

Getmantsev, G. G., N. A. Zuikov, D. S. Kotik, L. F. Mironenko, N. A. Mityakov, V. O. Rapoport, Yu. A. Sazonov, V. Yu. Trakhtengerts, and V. Ya. Eidman (1974), Combination frequencies in the interaction between high-power short-wave radiation and ionospheric plasma, *Sov. Phys. JETP, Engl. Transl.*, *20*, 101–102.

Gołkowski, M., and U. S. Inan (2008), Multistation observations of whistler mode chorus, *J. Geophys. Res.*, *113*, A08210, doi:10.1029/2007JA012977.

Helliwell, R. A. (1967), A theory of discrete VLF emissions from the magnetosphere, *J. Geophys. Res.*, *72*(19), 4773–4790.

Helliwell, R. A. (1988), VLF wave simulation experiments in the magnetosphere from Siple Station, Antarctica, *Rev. Geophys.*, *26*, 551–578.

Helliwell, R. A., and J. P. Katsufrakis (1974), VLF wave injection into the magnetosphere from Siple Station, Antarctica, *J. Geophys. Res.*, *79*(16), 2511–2518.

Helliwell, R. A., D. L. Carpenter, and T. R. Miller (1980), Power threshold for growth of coherent VLF signals in the magnetosphere, *J. Geophys. Res.*, *85*(A7), 3360–3366.

Inan, U. S., M. Gołkowski, D. L. Carpenter, N. Reddell, R. C. Moore, T. F. Bell, E. Paschal, P. Kossey, E. Kennedy, and S. Z. Meth (2004), Multi-hop whistler-mode ELF/VLF signals and triggered emissions excited by the HAARP HF heater, *Geophys. Res. Lett.*, *31*, L24805, doi:10.1029/2004GL021647.

Lehtinen, N. G., and U. S. Inan (2008), Radiation of ELF/VLF waves by harmonically varying currents into a stratified ionosphere with application to radiation by a modulated electrojet, *J. Geophys. Res.*, *113*, A06301, doi:10.1029/2007JA012911.

Moore, R. C., U. S. Inan, T. F. Bell, and E. J. Kennedy (2007), ELF waves generated by modulated HF heating of the auroral electrojet and observed at a ground distance of 4400 km, *J. Geophys. Res.*, *112*, A05309, doi:10.1029/2006JA012063.

Nunn, D. (1974), A self-consistent theory of triggered VLF emissions, *Planet. Space Sci.*, *22*, 349–378.

Omura, Y., H. Matsumoto, D. Nunn, and M. J. Rycroft (1991), A review of observational, theoretical and numerical studies of VLF triggered emissions, *J. Atmos. Terr. Phys.*, *53*, 351–368.

Piddyachiy, D., U. S. Inan, T. F. Bell, N. G. Lehtinen, and M. Parrot (2008), DEMETER observations of an intense upgoing column of ELF/VLF radiation excited by the HAARP HF heater, *J. Geophys. Res.*, doi:10.1029/2008JA013208, in press.

Platino, M., U. S. Inan, T. F. Bell, M. Parrot, and E. J. Kennedy (2006), DEMETER observations of ELF waves injected with the HAARP HF transmitter, *Geophys. Res. Lett.*, *33*, L16101, doi:10.1029/2006GL026462.

Rietveld, M. T., H. P. Mauelshagaen, P. Stubbe, H. Kopka, and E. Nielson (1987), The characteristics of ionospheric heating-produced ELF/VLF waves over 32 hours, *J. Geophys. Res.*, *92*(A8), 8707–8722.

Rietveld, M. T., P. Stubbe, and H. Kopka (1989), On the frequency dependence of ELF/VLF waves produced by modulated ionospheric heating, *Radio Sci.*, *24*, 270–278.

Sazhin, S. S., M. Hayakawa, and K. Bullough (1992), Whistler diagnostics of magnetospheric parameters: A review, *Ann. Geophys.*, *10*, 293–308.

Stiles, G. S., and R. A. Helliwell (1975), Frequency-time behavior of artificially stimulated VLF emissions, *J. Geophys. Res.*, *80*(4), 608–618.

Stubbe, P., H. Kopka, M. T. Rietveld, and R. L. Dowden (1982), ELF and VLF wave generation by modulated HF heating of the current carrying lower ionosphere, *J. Atmos. Terr. Phys.*, *44*, 1123–1135.

Strangeways, H. J., M. J. Rycroft, and M. J. Jarvis (1982), Multi-station VLF direction-finding measurements in eastern Canada, *J. Atmos. Terr. Res.*, *44*(6), 378–386.

Tsuruda, K., S. Machida, T. Teresawa, and A. Nishida (1982), High spatial attenuation of the Siple transmitter signal and natural VLF chorus observed at ground-based chain stations near Roberval, Quebec, *J. Geophys. Res.*, *87*(A2), 742–750.

M. B. Cohen, A. R. Gibby, M. Gołkowski, and U. S. Inan, STAR Laboratory, Department of Electrical Engineering, Stanford University, Packard Building, Stanford, CA 94305, USA. (mag41@stanford.edu)